J. Biochem. 127, 329–335 (2000)

Roles of Functional Loops and the C-Terminal Segment of a Single-Stranded DNA Binding Protein Elucidated by X-Ray Structure Analysis

Takashi Matsumoto,* Yukio Morimoto,* Naoki Shibata,* Takashi Kinebuchi,‡ Nobuo Shimamoto,‡ Tomitake Tsukihara,† and Noritake Yasuoka*,[1]

Department of Life Science, Himeji Institute of Technology, 3–2–1Kouto, Kamigori, Ako-gun, Hyogo 678–1297; †Institute for Protein Research, Osaka University, 3–2 Yamadaoka, Suita-shi, Osaka 565–0871; and ‡Structure Biology Center, National Institute of Genetics, Yata 1111, Mishima, Shizuoka 411–8540

Received October 22, 1999; accepted November 29, 1999

The single-stranded DNA (ssDNA) binding protein from *Escherichia coli* (*Eco*SSB) plays a central role in DNA replication, recombination, and repair. The tertiary structure of *Eco*SSB was determined at 2.2 Å resolution. This is rather higher resolution than previously reported. Crystals were grown from the homogeneous intact protein but the *Eco*SSB tetramer in the crystals contains truncated subunits lacking a part of the C-terminal. The structure determined includes biologically important flexible loops and C-terminal regions, and revealed the existence of concavities. These concavities include the residues important for ssDNA binding. An ssDNA can be fitted on the concavities and further stabilized through interactions with the loops forming flexible lids. It seems likely to play a central role in the binding of ssDNA.

Key words: crystal structure analysis, positive concavity, single-stranded DNA binding protein.

The single-stranded DNA (ssDNA) binding protein from *Escherichia coli* (*Eco*SSB) plays a central role in DNA replication, recombination and repair (*1–3*). *Eco*SSB is one of helix destabilizing proteins that are essential for DNA metabolism in all organisms, and binds tightly and co-operatively to ssDNA with little sequence specificity (*3*), but can also bind mRNAs with sequence specificity (*4*). However, *Eco*SSB cannot bind double-stranded DNA (*5*). It is believed to exist as stable homotetramers composed of subunits of 18,843 Da (*6*), which are considered to be the functional form (*7–10*). This tetramer can bind to ssDNA in several different modes (*11*, *12*), and its co-operativity is reduced at higher salt concentrations (*13*, *14*). To prove this idea, three distinct binding stoichiometries (35, 56, and 65 nucleotides per tetramer) were identified at different salt concentrations (*11*, *12*, *15*). Recently, two structures of *Eco*SSB have been reported, at resolutions of 2.9 Å (*16*) and 2.5 Å (*17*) (Table I). In one structure the L_{12} (Pro24–Gly27), L_{23} (Trp40–Lys49) loops, and the C-terminal region (Gly113–Phe177) were lacking (*16*), and in the other the L_{23} loop structure including important Trp40 could not assigned for ssDNA binding (*17*). Here we report the crystal structure of *Eco*SSB, at a higher resolution of 2.2 Å, including these loops and the C-terminal region. The newly solved structure, in conjunction with the results of a biochemical study on mutant proteins with deletions (*18*), has shed light on the structure–function relationship of the protein.

[1] To whom correspondence should be addressed. Tel: +81-791-58-0179, Fax: +81-791-58-0177, E-mail: yasuoka@sci.himeji-tech.ac.jp

MATERIALS AND METHODS

Purification and Crystallization of EcoSSB—*Eco*SSB was overproduced from pT7–7 and purified by the modified method described by Kinebuchi *et al.* (*18*), and then crystallized by the batch method with a protein concentration of 14 mg/ml. Into each glass vial was added 20 µl of precipitation solution (50 mM Tris-HCl, pH 9.0, 0.325 M NaCl, 0.3–0.6 M ammonium sulfate) and 20 µl protein solution, followed by standing at 4°C. Very small crystals appeared after two months. The glass vials containing small crystals were transferred to an incubator at 30°C. The small crystals were gradually dissolved in 24 h. The temperature was then decreased by 1°C per day until it reached 15°C. The prismatic crystals grew to dimensions of 1.0 mm × 0.3 mm × 0.3 mm.

Diffraction Experiments and Structure Determination—X-ray data were collected on the beamline ID14/EH3 at the European Synchrotron Radiation Facility (ESRF), and the beamline BL6A at the Photon Factory (PF) at room temperature. Diffraction data were recorded with an MAR CCD detector at the ESRF and a Fuji BAS-2000 image plate detector at the PF. Data sets were processed using the *HKL* package (*19*) and CCP4 suite (*20*). A molecular replacement method involving a partial model (*17*) yielded a clear solution in the cross-rotation function, translation search and rigid body refinement using the program X-PLOR (*21*). The initial $2F_o–F_c$ electron density was then refined by solvent flattening, histogram matching, and the NCS averaging technique using the program DM. A molecular envelope was generated with the programs NCSMASK and program MAMA in the O package (*22*). The sigma-weighted $2F_o–F_c$

TABLE I. **Summary of crystal data.**[a]

Matsumoto *et al.* (this work)	
Used protein	Native protein (177 residues)
Unit cell	105.37, 62.92, 97.79 Å, β=112.57°
Resolution	52.0–2.2 Å
R-merge[b]	5.9%
Resolution range	15.0–2.2 Å (*R*-factor[c] = 22.8%[d])
Assigned residues	576 residues
Raghunathan *et al.* (*16*)	
Used protein	Selenomethionyl chymotryptic fragment (135 residues)
Unit cell	58.0, 105.8, 90.2 Å, β=99.0°
Resolution	30.0–2.7 Å
R-merge	5.3%
Resolution range	8.0–2.9 Å (*R*-factor = 23.0%/*R*-free = 29.5%[e])
Assigned residues	384 residues
Webster *et al.* (*17*)	
Used protein	1 : 1 mixture of native and truncated protein (151 residues)
Unit cell	104.72, 62.19, 97.41 Å, β=112.63°
Resolution	30.0–2.5 Å
R-merge	16.9%
Resolution range	10–2.5 Å (*R*-factor=25.5%)
Assigned residues	412 residues

[a]These crystals belong to monoclinic space group *C*2. [b]*R*-merge: $\Sigma_h\Sigma_i|I(h,i)-\langle I(h)\rangle|/\Sigma_h\Sigma_i I(h,i)$, where $I(h,i)$ is the intensity value of the ith measurement of h, and $\langle I(h)\rangle$ is the corresponding mean value of $I(h)$ for all i measurements. [c]*R*-factor: $\Sigma||F_o|-|F_c||/\Sigma|F_o|$, where F_o and F_c are the observed and calculated structure factors, respectively. [d]No amplitude cutoff. No *R*-free reflections. [e]*R*-free was calculated using 10% of the reflections.

electron density map calculated with phases derived from this model was reasonably good within the model but unclear outside of it. Polypeptide chains were fitted into the electron density map with the program FRODO (*23*). Simulated annealing followed by positional and B-factor refinements was carried out with all data in 15–2.2 Å resolution with the program CNS (*24*).

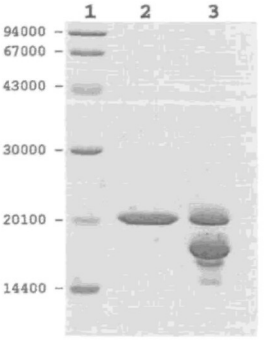

Fig. 1. **SDS-PAGE of purified *Eco*SSB used for crystallization and that recovered from crystals.** Proteins were stained with Coomassie Brilliant Blue R250. Three-fourths of *Eco*SSB in crystals lacked C-terminus ends, being truncated to give approximately 150 residues. The numbers to the left of the lanes denote the molecular weight markers (1), *Eco*SSB before crystallization (2), and dissolved crystals (3).

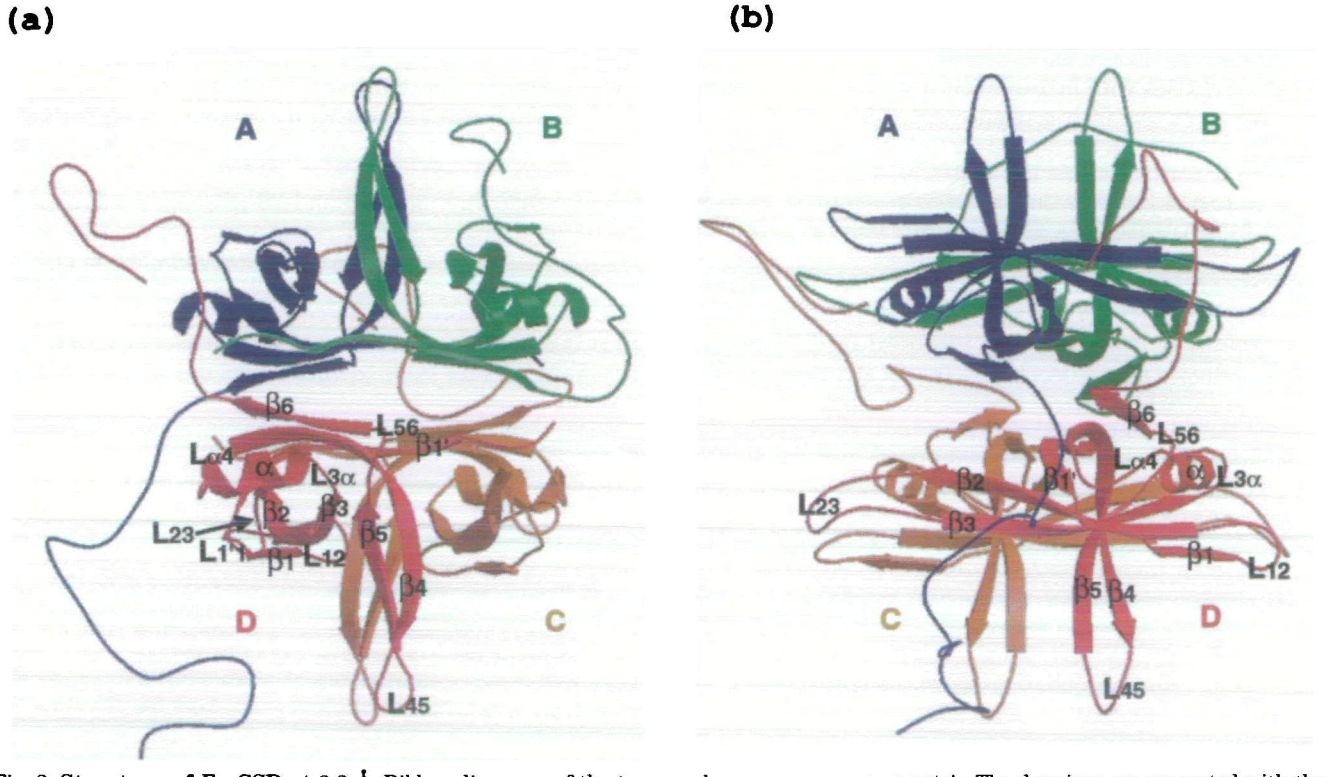

Fig. 2. **Structure of *Eco*SSB at 2.2 Å.** Ribbon diagrams of the tertiary structure of the *Eco*SSB tetramer. Monomers A (blue), B (green), C (orange), and D (red). The tetramer has a non-crystallographic 222 symmetry, but loops (L_{12}, L_{23}, and L_{45}) and the C-terminal region of each monomer are asymmetric. The drawing was generated with the programs FRODO and MOLSCRIPT (*29*). The view in (a) is orthogonal as to that in (b).

RESULTS

SDS-PAGE of Crystals—The purified *Eco*SSB before crystallization gave a single band on sodium dodecyl-sulfate polyacrylamide gel electrophoresis (SDS-PAGE) (Fig. 1). However, the protein recovered from crystals gave two major and two minor bands. The first major band corresponds to an intact protein, whereas the second major band and the two minor bands are due to truncated proteins. Quantitative analysis showed that the crystals were composed of an approximately 1 : 3 mixture of native (18.8 K) and C-terminal truncated polypeptide chains (16.5 K, 15.2 K, and 14.8 K). We tried to crystallize an intact *Eco*SSB tetramer, and we succeeded in getting crystals after two months. Judging from the SDS-PAGE results described above, truncation of the C-terminal regions of three chains within the tetramer might have occurred during this period. Since further purification by gel-filtration did not reveal any protease, the proteolysis may be autolysis. It is considered that the C-terminal parts of three subunits within a tetramer may be removed to decrease an unfavorable interaction for crystallization.

Structure of EcoSSB—The N-terminal part (Ala1–Met-111) of each monomer in the tetramer has an approximate (non-crystallographic) 222 symmetry (Fig. 2, a and b). But the C-terminal part (Leu112–) is not related by any symmetry element with any other part. The whole structure is composed of four monomers including about 30 residues newly assigned for C-terminal regions starting from Gly114 on the successive composite annealed omit maps in the CNS program. Figure 3 shows the amino acid sequence and schematic drawings of the secondary structure assigned, using *Eco*SSB nomenclature. The *Eco*SSB monomer

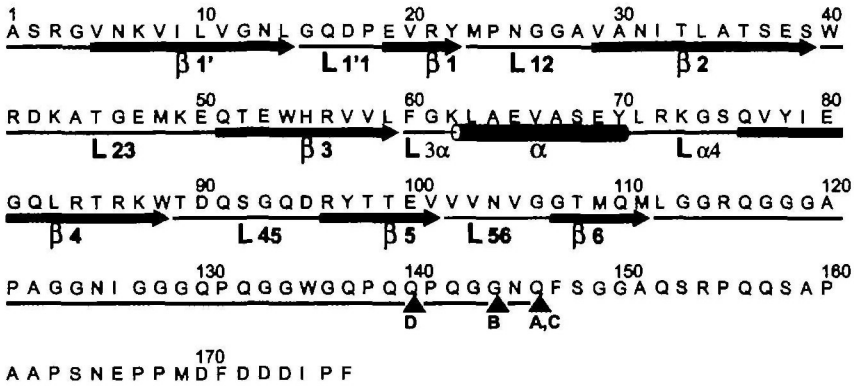

Fig. 3. **Schematic drawing of the secondary structure.** The structure-based sequence was generated using the program ALSCRIPT (*30*). The blue arrows and red bar show β-sheets and the α-helix, respectively. The assignment according to the OB fold rule (*31*) is shown in green. The limits of structure determination of monomers A to D are also shown (▲).

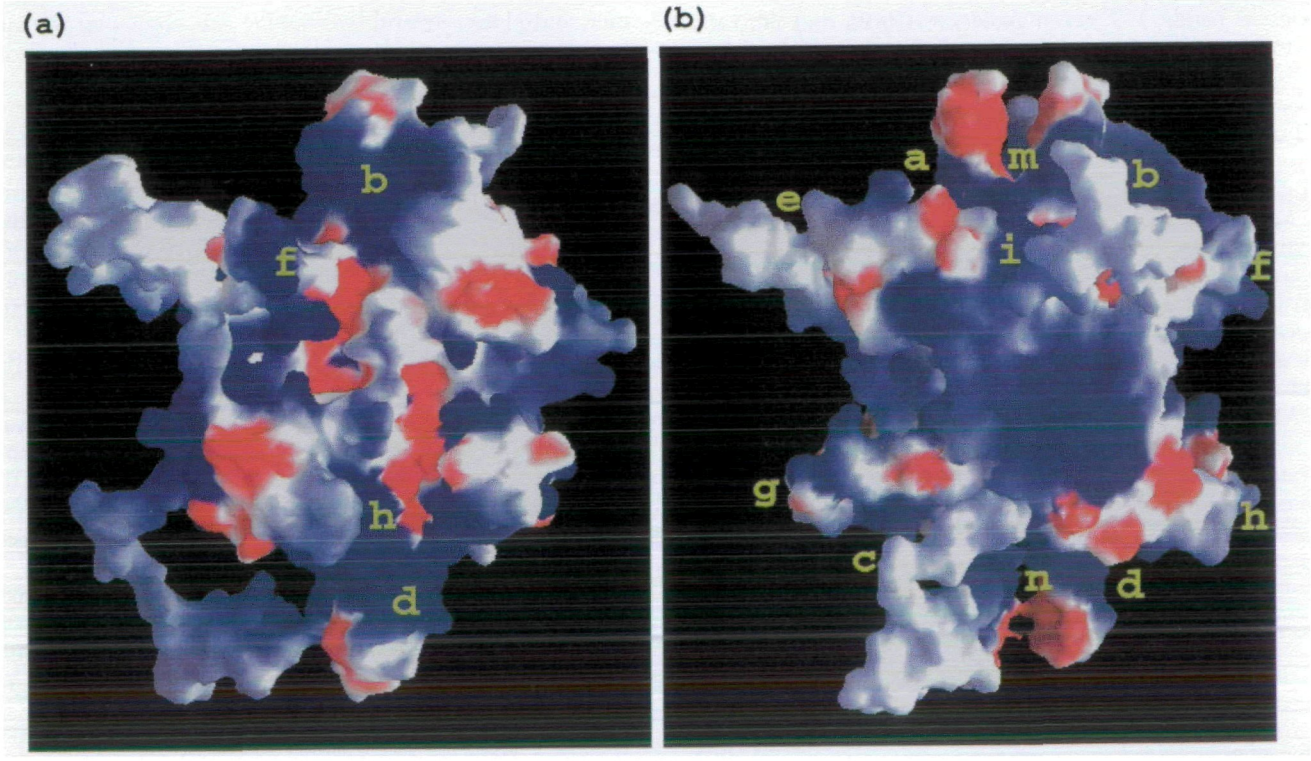

Fig. 4. **Electrostatic potential of the *Eco*SSB tetramer.** The views in Fig. 2a and Fig. 4a, and Fig. 2b and Fig. 4b are of the same orientation. Positive and negative potentials are shown in blue and red, respectively, using GRASP (*32*).

TABLE II. **Crystallographic data and statistics of structure refinement.**

Crystallographic data	
Space group	*C*2
Unit cell parameters	105.37, 62.92, 97.79 Å 90.0, 112.57, 90.0°
Resolution range	52.0–2.2 Å (2.37–2.20 Å)
Total number of reflections	150, 790
Number of unique reflections	24, 956
R-merge	5.9% (19.7%)
Completeness	82.7% (43.5%)
Overall multiplicity	6.0 (2.3)
Statistics of structure refinement	
Resolution range (Å)	15.0–2.2
Reflections used	24884
R-factor (%)	22.8
R.m.s.d from ideal bond lengths (Å)	0.0062
R.m.s.d bond ideal bond angle (deg)	1.20
Average B-factor (Å^2)	66.6
B-factor minimum/maximum (Å^2)	21.6/100.6
R.m.s.d B-factors	
Bonded main chain/bonded side chain (Å^2)	1.8/2.1
Angle main chain/angle side chain (Å^2)	3.2/3.0

TABLE III. **The naming scheme for the positive concavities observed on the surface of *Eco*SSB.** The amino acids and structural motifs such as β strands and loops constituting each concavity are listed.

Concavity	Amino acids, β strands and loops. A, B, C and D denote each monomer in the tetramer
a	A: Arg84, Arg21, β_1, β_2, β_3, β_4, β_5 B: Trp54, β_2, β_3
b	A: Trp54, β_2, β_3 B: Arg84, Arg21, β_1, β_2, β_3, β_4, β_5
c	C: Arg84, Arg21, β_1, β_2, β_3, β_4, β_5 D: Trp54, β_2, β_3
d	C: Trp54, β_2, β_3 D: Arg84, Arg21, β_1, β_2, β_3, β_4, β_5
e	A: Phe60, Arg3, Lys62, L_{12}, L_{3a}, L_{56} B: Trp40, Arg41, Lys43, L_{23}
f	A: Trp40, Arg41, Lys43, L_{23} B: Phe60, Arg3, Lys62, L_{12}, L_{3a}, L_{56}
g	C: Phe60, Arg3, Lys62, L_{12}, L_{3a}, L_{56} D: Trp40, Arg41, Lys43, L_{23}
h	C: Trp40, Arg41, Lys43, L_{23} D: Phe60, Arg3, Lys62, L_{12}, L_{3a}, L_{56}
i	A: Trp54, Arg56, Lys73, Arg72, $L_{1'1}$, L_{04}
j	B: Trp54, Arg56, Lys73, Arg72, $L_{1'1}$, L_{04}
k	C: Trp54, Arg56, Lys73, Arg72, $L_{1'1}$, L_{04}
l	D: Trp54, Arg56, Lys73, Arg72, $L_{1'1}$, L_{04}
m	A: Trp88, Lys87, Arg96, L_{45} B: Trp88, Lys87, Arg96, L_{45}
n	C: Trp88, Lys87, Arg96, L_{45} D: Trp88, Lys87, Arg96, L_{45}

has a total of 177 amino acid residues as an intact protein, however, in the figure three triangles indicate peptide terminals that we can trace for each monomer in the electron density map. Visible C-terminal regions are long and have no specific secondary structure. The structure has an *R*-factor value of 24.7% and an *R*-free one of 31.2% (*R*-free is calculated using 5% of the reflections; no amplitude cutoff). The final model has an *R*-factor value of 22.8% (no *R*-free reflections; no amplitude cutoff), including monomers A and C (Ala1–Gln146), B (Ala1–Gly144) and D (Ala1–Gln140), and 454 water molecules. The final model does not show large discrepancies from the standard geometry of peptide bonds, but seven residues (Gln94 and Gln140 of monomer A, Ser92 and Gln139 of monomer B, Lys43 and Leu112 of monomer C, and Gln94 of monomer D) fell in the disallowed regions of the Ramachandran plot. This structure has been deposited in the Protein Data Bank (accession code, 1QVC). The crystallographic data and refinement statistics are summarized in Table II.

Structure Comparison—We have compared our structure with the previously reported (*17*), in which the C-termini were not identified. Significant differences between the two structures were found mainly in loops L_{12}, L_{23}, and L_{45}. The overall r.m.s deviation of the main chain atoms of the two structures (Ala1–Gly107) is 3.35 Å. Within our structure, the conformations of loops L_{12}, L_{23}, and L_{45} are slightly different among the four monomers forming a tetramer.

Surface of EcoSSB—Positively charged concavities were found on the surface of the tetramer (Fig. 4, a and b). They may provide a hint as to the problem of how an ssDNA strand traces on the surface of *Eco*SSB. Each concavity extends over two different monomers except the concavities from **i** to **l**. The naming scheme for the positive concavities observed on the surface of *Eco*SSB is given in Table III.

DISCUSSION

Stabilization of Tetrameric Conformations—*Eco*SSB should form a tetramer for DNA binding, however, the deletion of residues Thr89–Val105 causes instability of the tetrameric structure of *Eco*SSB (*18*). Figure 5 shows the tetrameric form of *Eco*SSB and water molecules functioning as a paste between two monomers. The white chains are assigned as Thr89–Val105, this region of monomer A interacting with monomers B and C through the hydrogen bonds of water molecules, thereby stabilizing a tetramer. The N-terminal truncated mutant lacking Ala1–Val11 exists as an octamer (*18*). The Ala1–Val11 region forms an antiparallel β sheet with the same region of another monomer, and places several hydrophilic side chains on the surface of the tetramer. It is reasonable to predict the formation of a pile of two tetramers due to an interaction between otherwise exposed hydrophobic parts.

Function of the C-Terminal Region—Yuzhakov *et al.* (*25*) reported that the switching from priming to DNA polymerization at a replication fork is dependent on the C-terminal region. The present structure shows that the C-terminal region (Leu112–Gln146) protrudes from the rest of a tetramer, and that the four terminals have different conformations. The major interactions of the C-terminals with the surrounding molecules were found at Leu112–Gln146 of monomer A, Leu112–Gly144 of monomer B, Leu112–Gln146 of monomer C, and Leu112–Gln140 of monomer D. This unique structure suggests that the different interactions between the C-terminal regions (Leu112–Gln146) and surrounding molecules are weak. It is conceivable that the C-terminal region can move freely in solution helping *Eco*SSB interact with primase or the χ subunit of the clump loader (*25*).

Mechanism of ssDNA Binding—We recognized four positively charged concavities on the surface of *Eco*SSB, consisting of β-sheets, basic amino acids and loops. On C-terminal deletion up to Arg115 the affinity for ssDNA is retained, while deletion up to Val105 reduces the affinity by 100-fold, confirming a critical role of L_{56} containing Gly106–Arg115 in DNA binding (*18*). This suggests that concavities **e**, **f**, **g**, and **h** are required for ssDNA binding. It should be

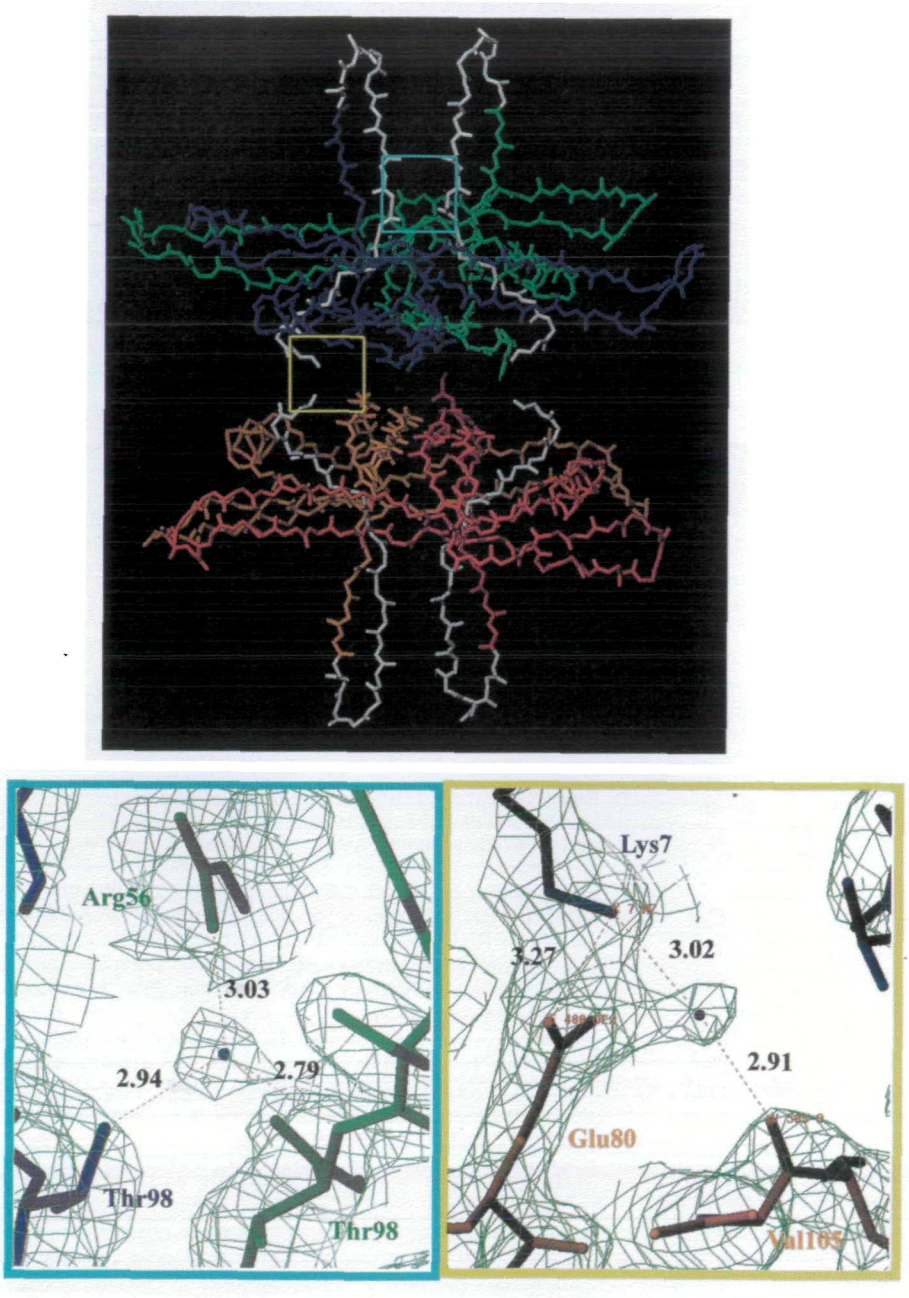

Fig. 5. **The region essential for the tetrameric form of *Eco*SSB.** The white chains are assigned as Thr89–Val105. The Thr89–Val105 region includes two specific hydrogen bond contacts *via* a water molecule between monomers. These hydrogen bond contacts function as a paste between monomers.

noted that the other three loops, L_{12}, L_{23}, and L_{45}, were found to have conformations constituting basic concavities **e**, **f**, **g**, **h**, **m**, and **n**. These loops contain positively charged side chains, which can interact with phosphates of ssDNA, and thus these loops may contribute to the binding to ssDNA. Although we have no structure for a DNA complex, the precise three-dimensional structure and its resultant surface potential may lead to the suggestion of a pathway and the interaction of *Eco*SSB with a single-stranded DNA wound around the tetramer. One idea is that *Eco*SSB may wind an ssDNA along a bent or crooked groove consist of six concavities in the sequence of **m**, **b**, **f**, **h**, **d**, and **n**.

Figure 6 shows biologically important tryptophan residues superimposed on the charged surface. The *Eco*SSB monomer has four tryptophan residues (40, 54, 88, and 135). Trp40, 54, and 88 play a central role in ssDNA binding (*26*), and Trp40 and Trp54 are important for the high affinity for ssDNA (*27*). These tryptophan residues are located on the positively charged concavities running over the interface between two monomers, furthermore, they could function beyond monomers. An indole ring of Trp40 located on loop L_{23}, newly found in this study, could be very important for a DNA wound around *Eco*SSB. It may be a holding or stacking force between the indole (Trp40) and aromatic (Phe60) rings located in loops L_{23} and $L_{3\alpha}$, respectively. The substitution of alanine for Phe60 results in a decrease in binding affinity by 3 orders of magnitude (*28*). Notably, all these important amino acids (Trp40, Trp54, Trp88, and Phe60) for ssDNA binding are located in these positively charged concavities.

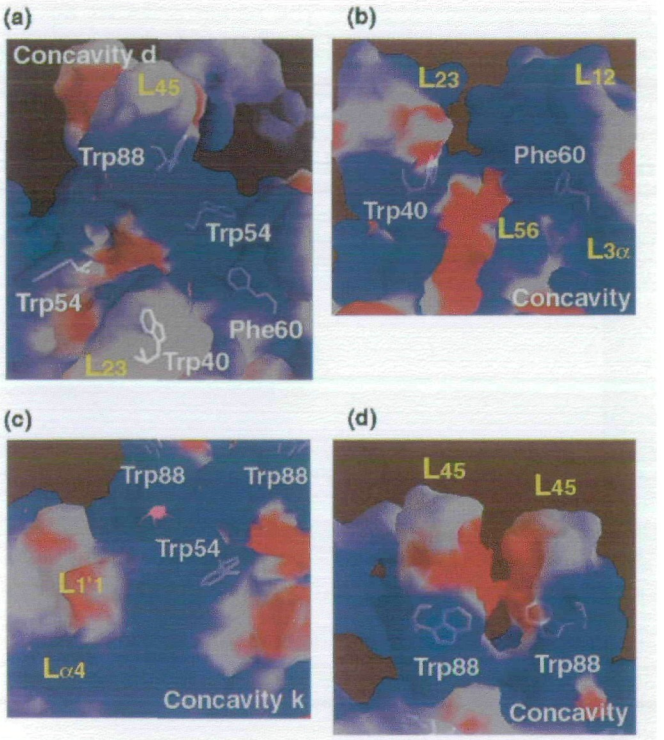

Fig. 6. **Locations of concavities, loops, and aromatic residues.** (a) Concavity d. (b) Concavity h. (c) Concavity k. (d) Concavity n. The figures were produced with GRASP. Four amino acids, Trp40, Trp54, Trp88, and Phe60, are important for ssDNA binding.

Sequenced Process of Binding of EcoSSB to ssDNA—The present structures may imply the interaction of *Eco*SSB with ssDNA in the following way. First, the loops rearrange on ssDNA binding so as to open the concavities. Then, four positive charge concavities, including Trp40, Trp54, Trp88, and Phe60, bind lagging ssDNA. Each loop catches ssDNA to further stabilize the complex. Finally, the C-terminal region interacts with primase or a clump loader.

We are grateful to Dr. R. Hilgenfeld for generously providing the *Eco*SSB coordinates. We are also thankful to Drs. W. Burmeister, T. Tomizaki, and S. Wakatsuki at ID14/EH3, Drs. J. Lescar, and B. Rasmussen at ID2 at the ESRF, and Dr. N. Watanabe, and Prof. N. Sakabe at BL6A at the PF for collecting the diffraction data.

REFERENCES

1. Chase, J.W. and Williams, K.R. (1986) Single-stranded DNA binding proteins required for DNA replication. *Annu. Rev. Biochem.* **55**, 103-136
2. Lohman, T.M., Bujalowski, W., and Overman, L.B. (1988) *E. coli* single strand binding protein: a new look at helix-destabilizing proteins. *TIBS* **13**, 250–255
3. Meyer, R.R. and Laine, P.S. (1990) The single-stranded DNA-binding protein of *Escherichia coli*. *Microbiol. Rev.* **54**, 342–380
4. Shimamoto, N., Ikushima, N., Utiyama, H., Tachibana, H., and Horie, K. (1987) Specific and cooperative binding of *E. coli* single-stranded DNA binding protein to mRNA. *Nucleic Acids Res.* **15**, 5241–5250
5. Weiner, J.H., Bertsch, L.L., and Kornberg, A. (1975) The deoxyribonucleic acid unwinding protein of *Escherichia coli*. Properties and functions in replication. *J. Biol. Chem.* **250**, 1972–1980
6. Sancar, A., Williams, K.R., Chase, J.W., and Rupp, W.D. (1981) Sequences of the *ssb* gene and protein. *Proc. Nal. Acad. Sci. USA* **78**, 4274–4278
7. Chase, J.W., Murphy, J.B., Whittier, R.F., Lorensen, E., and Sninsky, J.J. (1983) Amplification of *ssb-1* mutant single-stranded DNA-binding protein in *Escherichia coli*. *J. Mol. Biol.* **164**, 193–211
8. Williams, K.R., Murphy, J.B., and Chase, J.W. (1984) Characterization of the structural and functional defect in the *Escherichia coli* single-stranded DNA binding protein encoded by the *ssb-1* mutant gene. Expression of the *ssb-1* gene under lambda pL regulation. *J. Biol. Chem.* **259**, 11804–11811
9. Bujalowski, W. and Lohman, T.M. (1991) Monomers of the *Escherichia coli* SSB-1 mutant protein bind single-stranded DNA. *J. Mol. Biol.* **217**, 63–74
10. Bujalowski, W. and Lohman, T.M. (1991) Monomer-tetramer equilibrium of the ssb-1 mutant single strand binding protein. *J. Biol. Chem.* **266**, 1616–1626
11. Lohman, T.M. and Overman, L.B. (1985) Two binding modes in *Escherichia coli* single strand binding protein-single stranded DNA complexes. Modulation by NaCl concentration. *J. Biol. Chem.* **260**, 3594–3603
12. Bujalowski, W. and Lohman, T.M. (1986) *Escherichia coli* single-strand binding protein forms multiple, distinct complexes with single-stranded DNA. *Biochemistry* **25**, 7799–7802
13. Bujalowski, W. and Lohman, T.M. (1989) Negative co-operativity in *Escherichia coli* single strand binding protein-oligonucleotide interactions. I. Evidence and a quantitative model. *J. Mol. Biol.* **207**, 249–268
14. Bujalowski, W. and Lohman, T.M. (1989) Negative co-operativity in *Escherichia coli* single strand binding protein-oligonucleotide interactions. II. Salt, temperature and oligonucleotide length effects. *J. Mol. Biol.* **207**, 269–288
15. Bujalowski, W., Overman, L.B. and Lohman, T.M. (1988) Binding mode transitions of *Escherichia coli* single strand binding protein-single-stranded DNA complexes. Cation, anion, pH, and binding density effects. *J. Biol. Chem.* **263**, 4629–4640
16. Raghunathan, S., Ricard, C.S., Lohman, T.M., and Waksman, G. (1997) Crystal structure of the homo-tetrameric DNA binding domain of *Escherichia coli* single-stranded DNA-binding protein determined by multiwavelength X-ray diffraction on the selenomethionyl protein at 2.9-Å resolution. *Proc. Natl. Acad. Sci. USA* **94**, 6652–6657
17. Webster, G., Genschel, J., Curth, U., Urbanke, C., Kang, C., and Hilgenfeld, R. (1997) A common core for binding single-stranded DNA: structure comparison of the single-stranded DNA-binding proteins (SSB) from *E. coli* and human mitochondria. *FEBS Lett.* **411**, 313–316
18. Kinebuchi, T., Shindo, H., Nagai, H., Shimamoto, N., and Shimizu, M. (1997) Functional domains of *Escherichia coli* single-stranded DNA binding protein as assessed by analyses of the deletion mutants. *Biochemistry* **36**, 6732–6738
19. Otwinowski, Z. and Minor, W. (1997) Processing of X-ray diffraction data collected in oscillation mode in *Methods in Enzymology* (Carter Jr., C.W. and Sweet, R.W., eds.) Vol. 276, pp. 307–326, Academic Press, New York
20. Collaborative Computational Project, Number 4 (1994) The CCP4 suite: programs for protein crystallography. *Acta Cryst. D* **50**, 760–763
21. Brünger, A.T. (1987) A System for Crystallography and NMR, X-PLOR Manual-Version 3.1. Yale University Press, New Haven and London
22. Jones, T.A., Zou, T.T., Cowan, S.W., and Kjeldgaard, M. (1991) Improved methods for binding protein models in electron density maps and the location of errors in these models. *Acta Cryst. A* **47**, 110–119
23. Jones, T.A. (1985) Diffraction methods for biological macromolecules. Interactive computer graphics: FRODO in *Methods in Enzymology* (Carter Jr., C.W. and Sweet, R.W., eds.) Vol. 115, pp. 157–171, Academic Press, New York
24. Brünger, A.T., Adams, P.D., Clore, G.M., DeLano, W.L., Gros, P., Grosse-Kunstleve, R.W., Jiang, J.S., Kuszewski, J., Nilges, M., Pannu, N.S., Read, R.J., Rice, L.M., Simonson, T., and Warren,

G.L. (1998) Crystallography & NMR system: A new software suite for macromolecular structure determination. *Acta Cryst. D* **54**, 905–921
25. Yuzhakov, A., Kelman, Z., and O'Donnell, M. (1999) Trading paces on DNA—a three-point switch underlies primer handoff from primase to the replicative DNA polymerase. *Cell* **96**, 153–163
26. Curth, U., Greipel, A., Urbanke, C., and Maass, G. (1993) Multiple binding modes of the single-stranded DNA binding protein from *Escherichia coli* as detected by tryptophan fluorescence and site-directed mutagenesis. *Biochemistry* **32**, 2585–2591
27. Khamis, M.I., Casa-Finet, J.R., Maki, A.H., Murphy, J.B., and Chase, J.B. (1987) Investigation of the role of individual tryptophan residues in the binding of *Escherichia coli* single-stranded DNA binding protein to single-stranded polynucleotides. A study by optical detection of magnetic resonance and site-selected mutagenesis. *J. Biol. Chem.* **262**, 10938–10945
28. Casas-Finet, J.R., Khamis, M.I., Maki, A.W., and Chase, J.W. (1987) Tryptophan 54 and phenylalanine 60 are involved synergistically in the binding of *E. coli* SSB protein to single-stranded polynucleotides. *FEBS Lett.* **220**, 347–352
29. Kraulis, P.J. (1991) MOLSCRIPT: a program to produce both detailed and schematic plots of protein structures. *J. Appl. Crystallogr.* **24**, 946–950
30. Barton, G.J. (1993) ALSCRIPT: a tool to format multiple sequence alignments. *Protein Eng.* **6**, 37–40
31. Murzin, A.G. (1993) OB (oligonucleotide/ oligosaccharide binding)-fold: common structural and functional solution for non-homologous sequences. *EMBO J.* **12**, 861–867
32. Nicholls, A., Sharp, K.A., and Honing, B. (1991) Protein folding and association: insights from the interfacial and thermodynamic properties of hydrocarbons. *Proteins* **11**, 281–296